A great title

March 22, 2020

Introduction

The high biodiversity of plant communities is still an unresolved question for both experimental and theoretical ecologists. Both terrestrial plants and phytoplanktonic communities can present hundreds of species maintained by similar resources. Early theoreticians have proposed that environmental fluctuations only [ref] could sustain coexistence but further research showed that this could not explain the order of magnitude of species richness [ref]. Other mechanisms such as niche differentiation[ref], demography [ref] and life history traits [ref] have completed explanation by the stochastic environmental variations and demographic processes.

Analyses of coexistence in terrestrial plant communities often take into account several life stages [refs]. Considering at least two stages, seeds/juveniles and adults, different models have uncovered mechanisms that might explain long-term coexistence. Examples of such mechanisms are the bet-hedging strategy, the storage effect and the Janzen-Connell effect. Bet-hedging is a long-term strategy relying on the creation of seeds which can remain dormant for a long period of time (over a year, often much longer). Dormant seeds can tolerate harsher years during which adults cannot maintain, but they also reduce part of the population that could germinate from one year to another (in case of an annual plant). The storage effect has first been defined by the presence of a long-lived life stage and temporal variation in recruitment from this long-lived life stage that helps escape interspecific competition (Chesson, 1986; Cáceres, 1997). This has been later generalized as a negative correlation between the effect of the environment and the effect of competition (Ellner *et al.*, 2016). In good environmental conditions, competition between individuals is stronger as seeds might germinate and therefore use the same resources at the same time. Finally, models and experiments suggest that adults can have a negative effect on seed survival, through the Janzen-Connell effect (Comita *et al.*, 2014). Therefore, neglecting explicit modeling of this life stage can modify the understanding we have of the dynamics of the populations (Nguyen *et al.*, 2019).

Even though different coexistence mechanisms have been unveiled through the use of several life stages and a focus on the youngest stage (seeds) for terrestrial plants, aquatic plants, and more specifically phytoplanktonic algae, have not been modeled with the same precision. Although ecologists have proposed for a long time that the blooms (peaks in abundances that can cover several orders of magnitude) may initiate after the resuspension and germination of seeds (Patrick, 1948; Marcus & Boero, 1998), it is unusal to see an explicit model of such process (but see Hinners *et al.*, 2019). The classical view behind phytoplankton dynamics is that bloom formation is mostly seasonal, due to the variation in light and temperature, assuming vegetative cells remaining in the environment can duplicate enough to attain bloom amplitude. However, a recent review (Ellegaard & Ribeiro, 2018) suggests that seeds/cysts might another player .

Phytoplankton communities in coastal environments may benefit from seed banks even more than the oceanic communities [REF-find back], as the distance to the bottom is smaller. Also, and similarly to the seed bank approach in the terrestrial plant literature, Smayda (2002) has proposed the term "pelagic seed bank" to characterize

the contribution of the ocean to coastal communities. This has been noticed for dinoflagellate especially [[ref Dinophysis, check what we have on diatoms]]. Conversely, we can wonder to which extent the seed banks can contribute to the biodiversity in the ocean, especially in the long term. Indeed, spores are able to germinate again after tens of years (McQuoid *et al.*, 2002; Ellegaard & Ribeiro, 2018) or even thousands of years (Sanyal *et al.*, 2018) of dormancy, which can have a long-term effect on biodiversity in both oceanic and coastal environments.

Here we build on the work by Shoemaker & Melbourne (2016) and Wisnoski *et al.* (2019), as well as previous findings inPicoche & Barraquand (2019, 2020), to examine the effect of exchanges between different compartments (ocean and coastal water column and the bottom sediment) on coexistence.

Methods

Model

The model developed by Shoemaker & Melbourne (2016) and Wisnoski *et al.* (2019) builds on a two-step discrete-time model. First, coastal and oceanic cell numbers increase following Beverton-Holt (BH) dynamics (eq. 1). The BH formulation is classical for discrete-time models of terrestrial plants and includes a maximum achievable growth rate r which is modified by positive and negative interactions α_{ij}. As we assume that competition for nutrients is stronger in the ocean than along the coast [ref], a coefficient $k_{c2o} > 1$ is applied to competitive interactions and facilitation is removed from the oceanic interaction matrices. Here, the growth rate $r_i(T)$ varies with the temperature, and this variation depends on the genus of interest (see eq. 3). Abundances are also affected by a density-independent loss term l which can cover all other lethal processes such a natural mortality or predation. During the same first step, the abundance of cells present at the bottom of the water column in coastal areas (hereafter called cysts) decreases with cyst mortality (m) and burial resulting from sedimentation (ζ).

$$\begin{cases} N_{t+h,i,c} &= \frac{e^{r_i(T)}N_{t,i,c}}{1+\sum_j \alpha_{ij}N_{t,j,c}} - lN_{t,i,c} \\ N_{t+h,i,o} &= \frac{e^{r_i(T)}N_{t,i,o}}{1+k_{c2o}\sum_j \alpha_{ij}N_{t,j,o}} - lN_{t,i,o} \\ N_{t+h,i,b} &= N_{t,i,b}(1-m-\zeta) \end{cases} \tag{1}$$

Second, exchanges take place between the three compartments (eq. 2).

$$\begin{cases} N_{t+1,i,c} &= N_{t+h,i,c}(1-s_i-e) + \gamma N_{t+h,i,b} + eN_{t+h,i,o} \\ N_{t+1,i,o} &= N_{t+h,i,o}(1-s_i-e) + eN_{t+h,i,c} \\ N_{t+1,i,b} &= N_{t+h,i,b}(1-\gamma) + s_i N_{t+h,i,c} \end{cases} \tag{2}$$

Parameters and state variables are defined in Table 1.

Param	Name	Value (unit)
$N_{t,i,c/o/b}$	Abundances of species i at time t in the coast (c) or ocean (o) water column, or in the benthos (b)	NA (Number of cells)
T	temperature	NA (K)
$r_i(T)$	growth rate of species i	NA
b_i	Normalization constant for the thermal decay rate	(K^3)
τ_0	Reference temperature	293 (K) / 20 (°C) (Scranton & Vasseur, 2016)
$a_r(\tau_0)$	Growth rate at reference temperature	$386(\frac{\text{kg}}{\text{kg} \times \text{year}})$ (Scranton & Vasseur, 2016)
E_r	Activation energy	0.467 (eV) (Scranton & Vasseur, 2016)
$T_{\min}$	Minimum thermal optimum	0
$T_{\max}$	Maximum thermal optimum	30 (approximate of the range in Edwards *et al.* (2016)
T_i^{opt}	Optimal temperature for species i	Adapted from Picoche & Barraquand (2020)
$\alpha_{ij,c/o}$	interaction strength of species j on i	Adapted from Picoche & Barraquand (2020)
k_{c2o}	conversion coefficient from coastal to oceanic interactions	1.5 [arbitrary]
A_i, b_i	Niche area, width	NA
g	gain in growth rate	0.2 [this study, based on Edwards *et al.* (2016)]
s_i	sinking rate of species i in a coastal environment	$\{0.1; 0.3; 0.5\}\beta(0.55, 1.25)$ (Passow, 1991)
e	exchange rate between ocean and coast	$\{0.4 ; 0.6 ; 1\}$ (Ascione Kenov *et al.*, 2015)
l	loss of vegetative phytoplankton (predation, mortality...)	0.04 (Scranton & Vasseur, 2016)
m	cyst mortality	$\approx 10^{-4}/10^{-5}$(McQuoid *et al.*, 2002)
ζ	cyst burial	$\{0.01 ; 0.1 ; 0.3\}$ [arbitrary]
γ	germination $\times$ resuspension rate of species	$\{0.1;0.01;0.001\} * \{10^{-5},0.1\}$ [abitrary]

Table 1: Definition of main variable states and parameters of the model. Fixed values or distributions are estimated from the literature. When a set or a range of values is given, the sensitivity of the model related to changes in parametes has been assessed (see text).

More precisely, in eq. 1, the coefficients α_{ij}, i.e. the strength of the effect of species j on species i for all i and j, are inferred from a previous work on coastal data with a Multivariate AutoRegressive (MAR) model (Picoche & Barraquand, 2020). The shift from MAR to BH- interaction matrices is described in SI. The change in growth rate $r_i(T)$ is based on the formula by Scranton & Vasseur (2016) (eq. 3).

$$r_i(T) = a_r(\tau_0)e^{E_r \frac{(T-\tau_0)}{kT\tau_0}} f_i(T) + g$$

$$\text{where } f_i(T) = \begin{cases} e^{-|T-T_i^{opt}|^3/b_i}, & T \leq T_i^{opt} \\ e^{-5|T-T_i^{opt}|^3/b_i}, & T > T_i^{opt} \end{cases}$$

$$\text{and} \quad b_i \text{ is defined by numerically solving} \quad \int r_i(\tau)d\tau = A_i \tag{3}$$

In this model, species are therefore defined by their thermal optimum T_i^{opt}. The equation by Scranton & Vasseur (2016) was modified to account for two more processes. Taxa roughly divide between generalists and specialists, with more or less tolerance to variations in the temperature. Generalists have a larger niche width than specialists, which can be roughly translated by a larger A_i (for more details on the modeling of generalist and specialist, see specific section in SI). Field-based estimation of the niche area A_i is described in the next section. However, apart from a radical and unrealistic change in A_i value, the resulting growth rate decreases very rapidly with the distance from T_i^{opt}, leading to values close to 0 for temperatures in which phytoplankton can normally grow. The meta-analysis by Edwards *et al.* (2016) can be used to correct at least qualitatively the growth rate for temperature outside the range of the considered taxa, by adding a gain g in the final growth rate (see a comparison of the original and final versions of the growth rates in SI, Fig. S6).

Finally, the temperature at each time step is a repetition of the temperatures observed over 20 years in our example dataset.

Each compartment (ocean, coast, seed bank) contains 10^3 cells at the beginning of the simulation, which is run for 10000 time steps.

Parameterisation

Data set example

Parameter values

Phenology In eq. 3, the growth rate is mainly defined by two parameters: the thermal optimum T_i^{opt} and the niche area A_i, which drive the phenology of the genus. Each year, the dynamics of phytoplanktonic organisms is characterized by a blooming period and a lower concentration during the rest of the year. The bloom can be triggered by a combination of nutrient and light input, as well as a sufficient temperature. All parameters being more or less dependent on seasonality, it is reasonable to restrain this study to the effect of temperature.

We base estimates of T_i^{opt} and A_i on field observations. For each genus and each year, the beginning of the bloom of a given genus is defined by the date at which its abundance exceeds its median abundance over the year. The duration of the bloom is the number of days between the beginning and the date where abundance fall below the median value. Generalists are characterized by one long bloom in the year or several blooms when the abundances oscillate around their median. Specialists tend to appear only once or twice in the year for shorter amounts of time. A genus is therefore defined as a generalist if its cumulated blooms cover at least a third of the year (122 days) for at least 15 years over the 20 years of the time series.

With these values in mind, we can define two range of values for the niche width (5-10 for specialists, 12-17 for the generalists) and then order the species in these ranges as a function of the mean sum of their bloom length, i.e. $\sum \overline{L}_{i,b} > \sum L_{j,b} \Rightarrow A_i > A_j$ where $\overline{L}$ is the mean over 20 years of the annual cumulated lengths of the bloom.

The thermal optimum T_i^{opt} is defined as the mean minimum value of the temperature at the beginning bloom throughout the whole time series.

Mortality The loss rate of vegetative cells is defined according to Scranton & Vasseur (2016). It could however be turned into a delayed, density-dependent mortality to take into account phenomena such as predation (simplest form: $lN_{t-\tau,i,o/c}$ where τ is the necessary lag between phytoplanktonic growth and predator response, for instance [look for ref, Reynolds not helpful here]).

Sinking rate Phytoplanktonic particles have a higher density than water and cannot swim to prevent sinking (although see Reynolds (2006) for a discussion on the settling of phytoplanktonic cells compared to inorganic particles). The sinking rate of vegetative cells depends mostly on their size and shape, and can also be affected by their capacity to form colonies. Sinking is also affected by hydrodynamics: more turbulence and eddies can retain the cells at the top of the water column. In field conditions (Gotland Basin in central Baltic Sea), Passow (1991) measured a large variability in sinking rates, even within the same genus (e.g., between 1 and 30% for *Chaetoceros* spp.). However, a pattern could be distinguished, with a small number of genera that sinked more than the rest of the community. The mean rate for *Chaetoceros* and *Thalassiosira* was around 10% while it was around 1% for the other species. Sinking rate values around 10% are consistent with the loss rate values in Kowe *et al.* (1998) in a river and Wiedmann *et al.* (2016) in an estuary (mouth of Adventfjorden).

An arbitrary beta distribution was selected, with a mean value close to the ones observed in both papers (between 9 and 10), and a maximum around 30%, that is $s \backsim 0.3\beta(0.55, 1.25)$ (see Fig. S5).

However, it should be noted that the sinking rate measured in these two articles represent the sinking of all cells, therefore including dead cells. In our model, it should represent the exchange of live cells between the coast and the seed bank, or a loss of cells in the ocean. Our sinking rate might therefore need to be decreased to avoid modeling dead cells already taken into account in the loss term.

Exchange rate The exchange rate between the ocean and the coast depends on the shape and location of the estuary. In Marennes-Oléron and more specifically in Auger, the renewal time is very short, between 1 and 2.5 days (Ascione Kenov *et al.*, 2015), which correponds to a daily rate between 40 and 100 %.

Cyst mortality and burial Cyst loss is a composite of cyst mortality m and inaccessibility ζ. McQuoid *et al.* (2002) provide species-specific values of mean and maximum depths at which cysts can still germinate. Corresponding mortality values range between 10^{-5} and 10^{-4} (more details on the approximation of mortality rates are given in SI). However, cyst burial by sedimentation[1] might be a prevailing phenomenum in driving phytoplanktonic dynamics. Once cysts have been buried, they are not accessible for resuspension even if they could have germinated. Burial depends on the hydrodynamics of the site, but also on biotic processes (i.e., bioturbation) and anthropogenic disturbances such as fishing or leisure activities (e.g., jet skiing). This parameter is thus heavily dependent on the environmental context we wish to describe.

Germination/resuspension Germination and resuspension might be difficult to differentiate as they are finally gathered in only one parameter (γ = resuspension$\times$germination).

The germination process has been studied a lot. From McQuoid *et al.* (2002) Agrawal (2009), we can assume that there is a temperature threshold for germination. Eilertsen *et al.* (1995) also present an effect of photoperiodicity but this can be mingled with seasonal variation in temperature. In this model, germination is triggered by temperatures going above 15°C. As rates are not easily deduced from the literature, arbitrary values are fixed (1%, 0.1%, 0.01%) and the effect of their variation on the simulations is assessed.

Resuspension values are seldom computed for phytoplanktonic cells, but models for other particles such as sediments can be used. Rates vary from one publication to another: in Fransz & Verhagen (1985) in a coastal area, resuspension rate of sediments is evaluated around 5.10^{-5} day^{-1} in winter and decreases in summer, with a link between resuspension and light extinction coefficient. In Kowe *et al.* (1998), the resuspension rate of diatoms is evaluated around $1.9.10^{-5}$ day^{-1}. In Le Pape *et al.* (1999), resuspension rate of sediments and dead diatoms is 0.002 day^{-1}. In this paper, we explore values between 10^{-5} (stratified water column) to 0.1 (highly mixed environment).

Finally, it should be noted that cyst burial, sinking rate and resuspension are all dependent on the hydrodynamics of the place and are therefore, at least in biological terms, not identifiable.

Parameter calibration

Maynard *et al.* (2019) recently applied quadratic programming (Bazaraa *et al.*, 2013) to ecological data, which improved the calibration of certain parameters and led to more realistic simulations. Even though we could directly use the values obtained in the literature and in previous studies (Picoche & Barraquand, 2020), the switch from a fifteen-day MAR model to a daily BH-model and the high uncertainty for all parameters due to the use of proxies, and high variability in phytoplanktonic genera on their own, are motivations to calibrate the model more precisely. Following the example of Maynard *et al.* (2019) with the package limSolve in R [ref, version], we intend[2] to apply quadratic programming to our interaction matrices. Contrary to Maynard *et al.* (2019), we do not broaden the calibration process to growth rates as ours are not fixed values in a linear model.

Sensitivity analysis As mentioned above, several parameters are site-specific and the effect of a change in parameter values needs to be evaluated. The sinking, resuspension/germination and burial rates are the parameters to evaluate. The range of probable values for each parameter, and more specifically the set of values to be tested,

---

[1] Any idea for a better way to call it than burial?

[2] I use this term because I am really not sure this is what we want to keep. I need to know how this method can be applied to cycles.

is given in Table 1. The main diagnostics are the final mean abundance, amplitude and timing of the bloom (peak in abundance) for each genus.

For each combination of values, the diagnostics are performed on the last year of the simulation and the variability of theses diagnostics with respect to each parameter is determined, as well as the best fit to real data.

Scenarios

Maintenance of biodiversity by exchanges between compartments can be gauged with two main scenarios.

1. modifying the storage of cysts in seed bank (by setting seed mortality/burial to 1)

2. changing the exchanges between the coast and the ocean (e=0)

Final richness and average abundance/biomass productivity (approximated by the final total abundances, to create a link with ecosystem functions) can be diagnostics.

We can make 2 a-priori hypotheses. First, removing the seed bank would increase the sensitivity to competition, i.e. decrease the maximum sustainable interspecific competition strength, and decrease the resilience of the community confronted to changes in the environment. (Fig. 1). Under high competition, variability in final richness may increase because exclusion is more likely, especially without a seed bank. This is also true for higher temperatures.
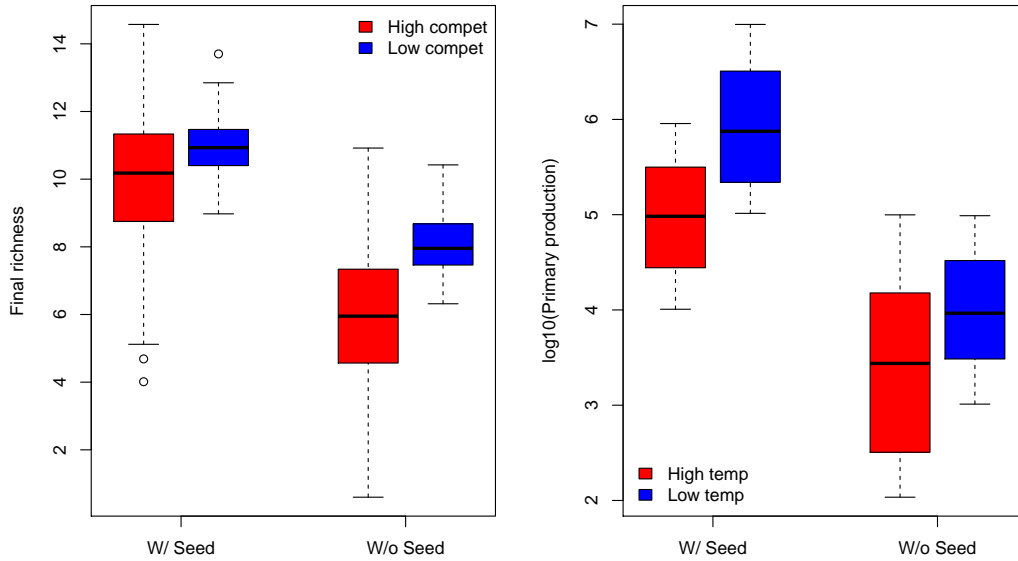

Figure 1: Expected changes in the model outputs in the ocean. Left panel, final richness with and without seed bank, with high (red) and low (blue) interspecific competition. Right panel, final primary productivity with and without seed-bank, with a high (red) and low (blue) mean temperature.

Second, by reducing the exchange with the ocean might end up depleting the ocean biomass and richness as it loses species by sinking but cannot regain them thanks to coastal production fueled by a seed bank. Fig. 2 gives a more precise view of the possible interactions of seed mortality and exchange between the coast and the ocean.
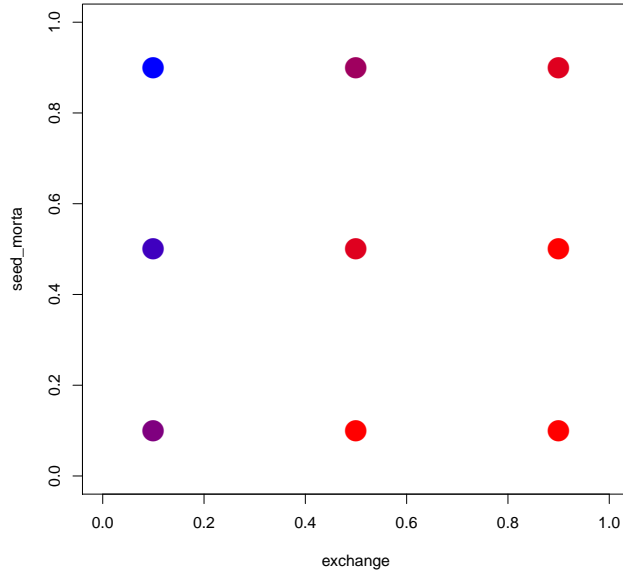
Figure 2: Expected changes in community richness in the ocean for different values of seed mortality/burial (=access to the seed compartment) and exchange with the ocean. Point color indicates final richness in the ocean, from low (blue) to high (red).

Results

Quadratic programming

Using quadratic programming (see SI) as a way to tune interaction strengths on the observed abundances leads to changes in parameter values (Fig. 3). Some interactions can be multiplied by 40 after re-calibration (LEP/GUI) while most of the parameters at least keep their order of magnitude.
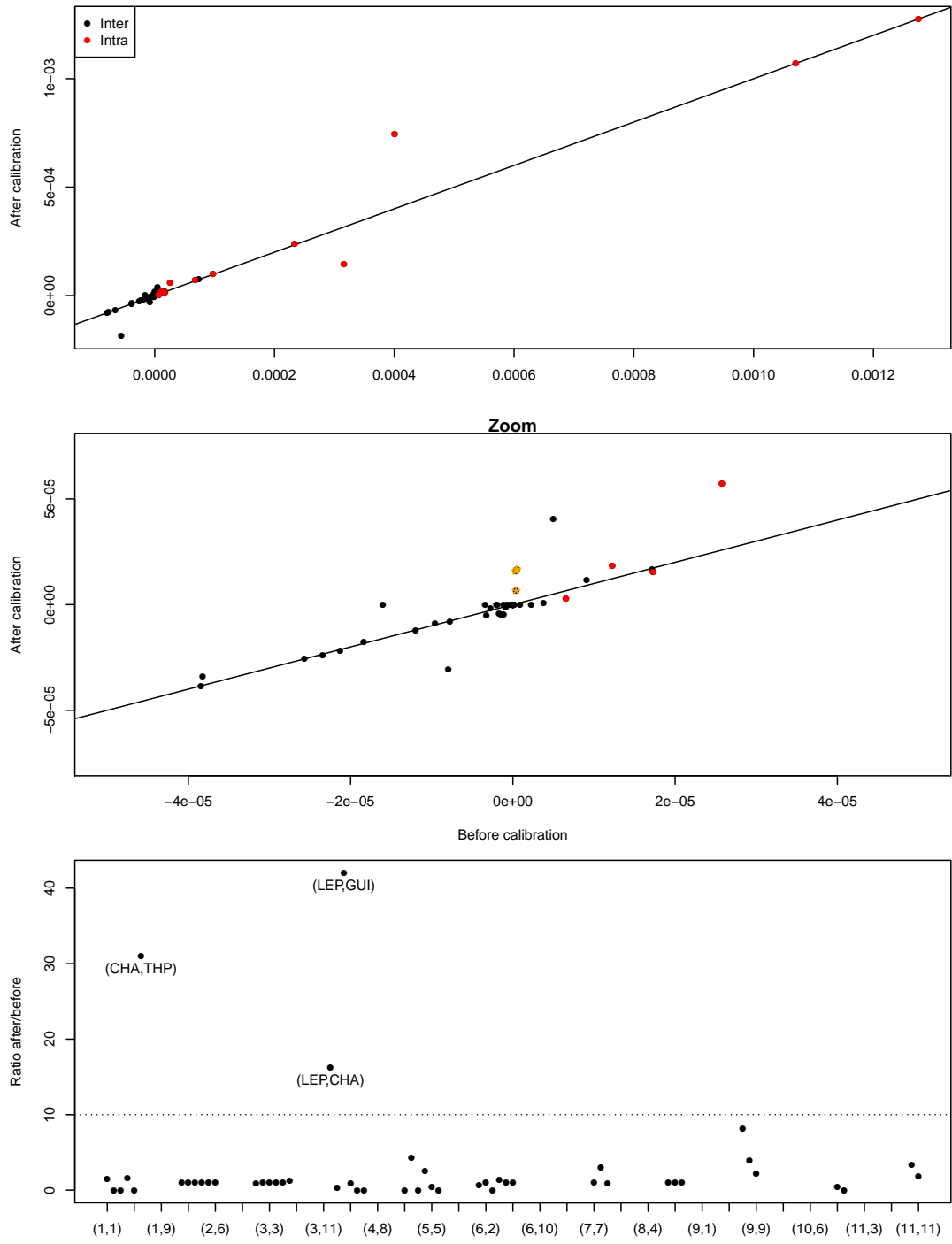
Figure 3: Changes in interaction strengths after calibration by quadratic programming. The middle panel is a zoom on interspecific interaction strengths presented in the top panel. Orange stars show the interactions for which the ratio of values before and after calibration is the higher, i.e. above 10. The bottom panel shows the ratio of parameter values after and before quadratic programming, with a dotted line showing a threshold at 10.

Phytoplankton dynamics

There are still issues in the calibration of the model: abundances can be lower than expected and the variation in abundances due to seasonality is, for now, underestimated (Fig. 4). [3]
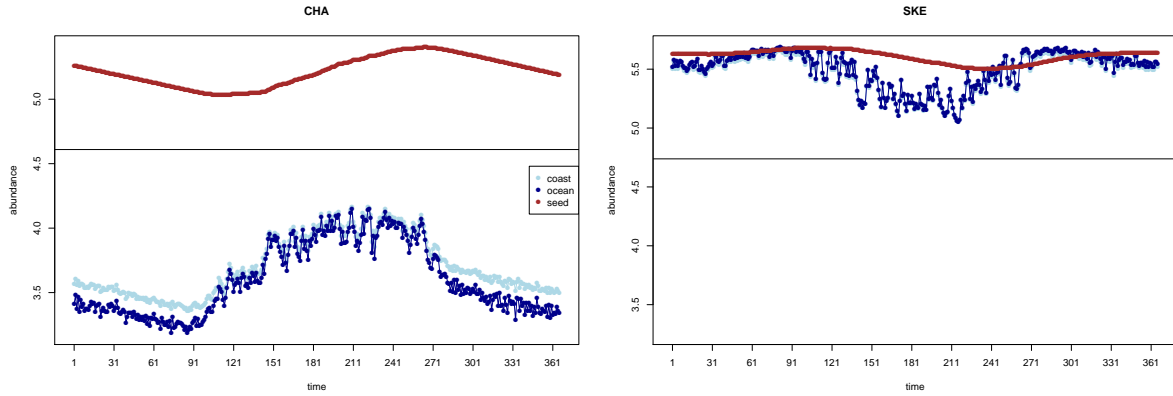

Figure 4: Examples of phytoplankton dynamics (*Chaetoceros* on the left, *Skeletonema* on the right). The solid black line is the observed average abundance of the species.

Discussion
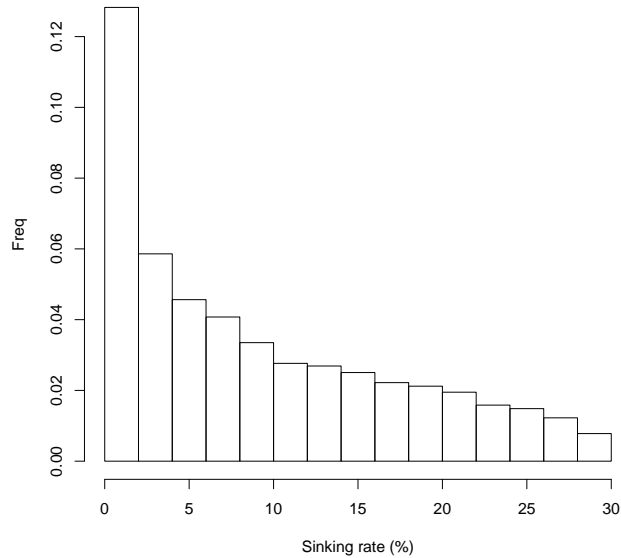
Supplementary Information

Sinking rate distribution

Figure 5: Possible beta-distribution of sinking rates

---

[3]WARNING: This was not done with an updated phenology

Growth rate: variation with temperature

Phytoplanktonic growth rates are highly variable, in situ or in experimental conditions. An example of such variability appears in Balzano *et al.* (2011). For ten strains of one genus only (*Skeletonema*), and in the same experimental conditions, Balzano *et al.* (2011) have been able to detect growth rates between 0.5 and 1.25 day^{-1}, which corresponds more generally to the values found in the literature (between 0.2 and 1.78 for diatoms in Reynolds (2006), even reaching 3 in the meta-analysis of 308 experiments by Edwards *et al.* (2015); this can be much lower for dinoflagellates). These growth rates are maximum, fixed values for isolated species in laboratory conditions. Most of the time, they correspond to fixed temperature conditions, or to only a small set of values. These observations therefore cannot accomodate realistic, seasonal environment.

In this context, Bissinger *et al.* (2008) based their study on a seminal work by Eppley (1972) to compute the maximum possible growth rate depending on the temperature. The relationship between temperature and maximum growth rate, evaluated on a large database, is then $r(T) = 0.81\mathrm{e}^{0.0631T}$, with T in °C. In this case, growth rates vary between 0.81 and 3.9 day^{-1} for temperatures between 0 and 25°C, in line with previous observations. However, these values only illustrate a maximum, exponential growth which cannot be realistic for species with different niche temperatures.

The equation of Scranton & Vasseur (2016) distinguishes different niches based on optimal temperature. However, it needed to be modified to be closer to the shape in other works (Eppley, 1972; Bissinger *et al.*, 2008; Edwards *et al.*, 2016).
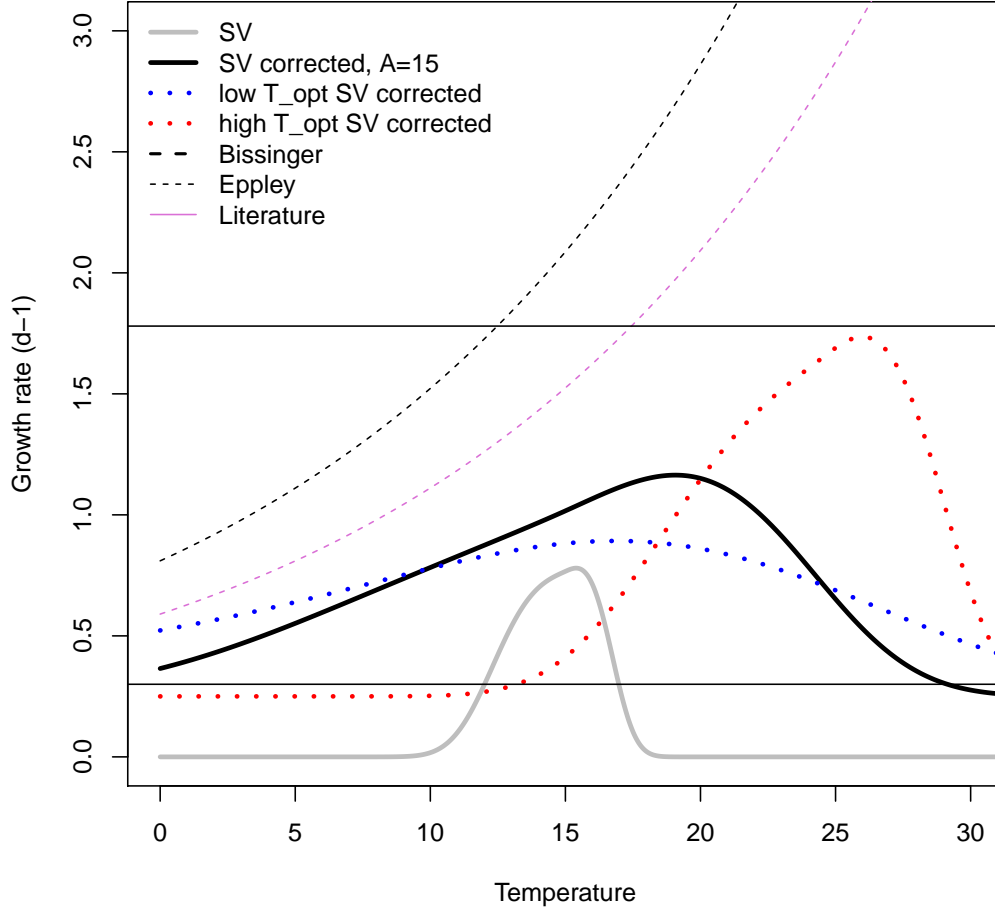
Figure 6: Comparison of growth rate formula. The SV solid grey line corresponds to the original Scranton and Vasseur (2016) formula. The solid black line includes both a new niche area and a gain in growth rate, and the shape of the growth rate as a function of temperature is given for a low (blue) and high (red) values of thermal optimum with dotted lines. The Bissinger and Eppley lines correspond to the formula of maximum growth rates in the studies from eponymous authors. Finally, horizontal lines show limits taken in the literature.

Growth rate: generalists vs specialists

From eq. 3, let us note $r_i(T) = a_r(\tau_0)e^{E_r \frac{(T - \tau_0)}{kT\tau_0}} f_i(T) = E(T)f_i(T)$. Hereafter, we will call $f_i(T)$ the niche part of the equation and $E(T)$ the metabolism part. The metabolism part is driven by both metabolism theory ecology and by observations in Eppley (1972) study of maximum growth rates for phytoplankton.

The simplest way to define generalists and specialists is to remove the constraint on the fixed niche area A. In this case, the only parameter that defines the niche width is b. However, increasing b does not only lead to increases in niche width, but also to a shift towards larger values to attain the maximum growth rate. This means that for the same theoretical T_i^{opt}, the observed thermal optimum is higher.
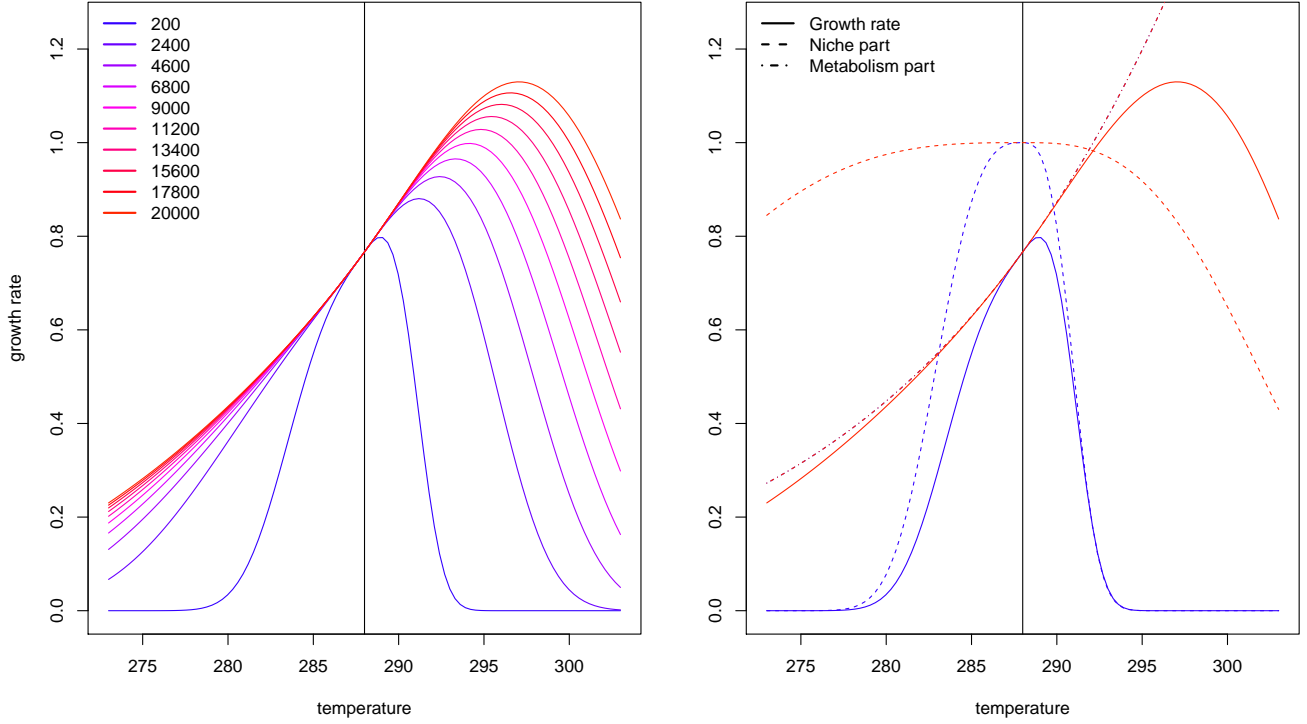
Figure 7: Relationship between daily growth rates and temperature with different values of niche width b (whose values are indicated in the legend) and the same thermal optimum, 15°C, indicated by the solid black. In the left panel, only the two extreme values of b (200 and 20 000) are shown in blue and red respectively. Coloured lines then correspond to the final growth rate, dashed lines correspond to $f_i(T)$ values (see eq. 3) and dotted lines correspond to $E(T)$ values.

When b increases, the niche term f_i shows smaller variations in values around the thermal optimum and the final value of the growth rate is driven by the metabolism part of the equation. This can lead to confusions on the observed thermal optimum that we wish to obtain.

Even if we only keep the maximum growth rate computed in Bissinger *et al.* (2008) (as an update of Eppley's curve), we obtain slightly higher growth rate values but the same shift.
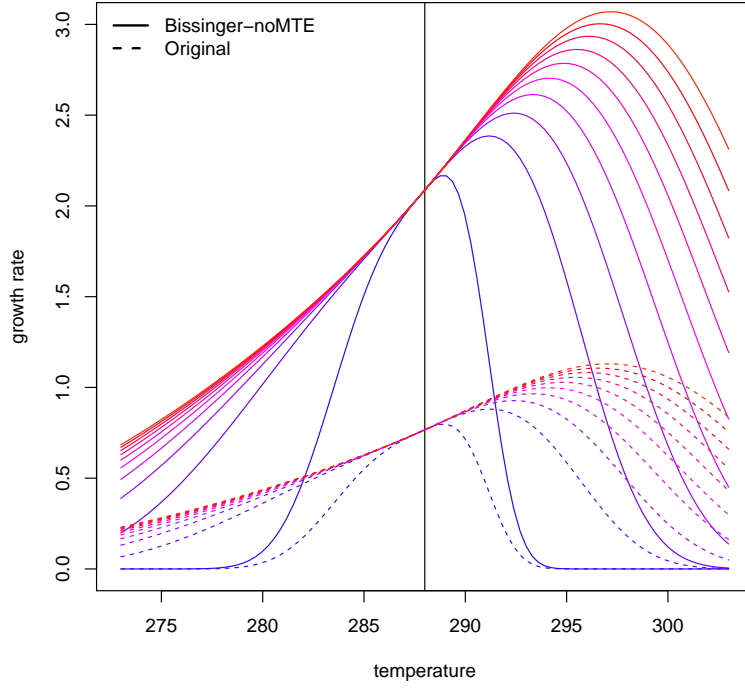
Figure 8: Relationship between daily growth rates and temperature with different values of niche width b (legend for the values of b is give in the figure above). Dashed lines correspond to the original formulation of Scranton & Vasseur (2016) while solid lines correspond to a formulation of the temperature-dependent maximum growth computed in Bissinger *et al.* (2008).

The control over the width, height and location of the niche is not obvious with the realistic Scranton & Vasseur (2016) model. In addition to this lack of control, specialists present in our dataset tend to bloom at lower temperatures (spring and sometimes autumn), which would mean they would have both a smaller and more narrow niches.

A toy-model would allow us to have more control on the width and height, see other possibilities in Fig. S9.
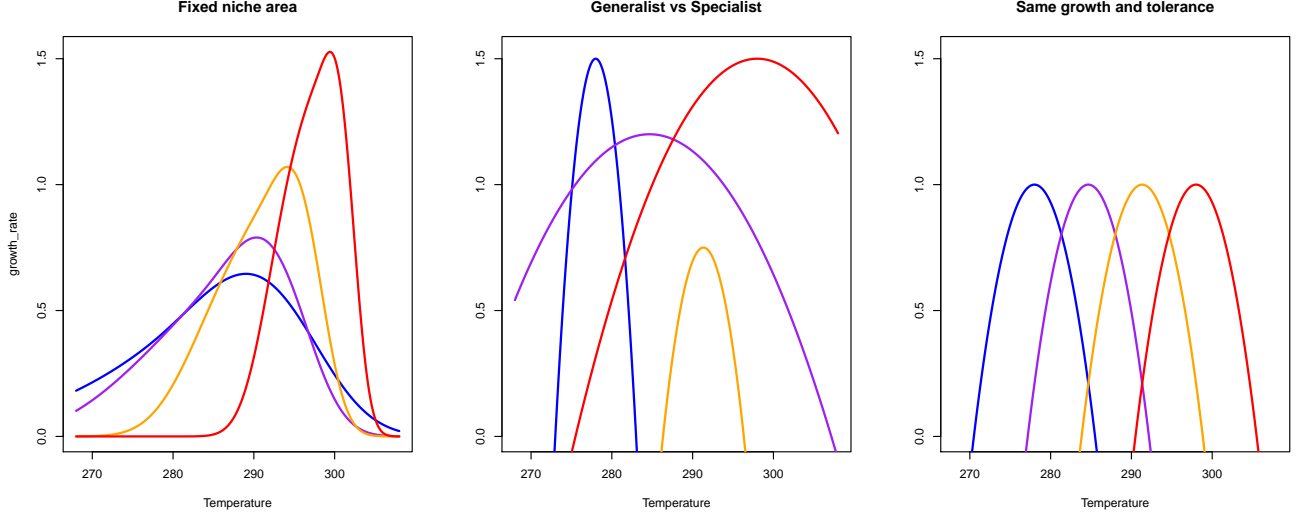
Figure 9: Example of simplistic niche shapes we could use.

Community matrix: correspondence between Multivariate Autoregressive and Beverton-Holt models

Certain *et al.* (2018) showed that MAR and BH interaction coefficients, respectively b_{ij} and α_{ij}, could map once abundances at equilibrium N_i^* are defined.

$$\begin{cases} b_{ii} - 1 = & \frac{-\alpha_{ii} N_i^*}{1 + \sum_l \alpha_{ij} N_l^*} \\ b_{ij,i \neq j} = & \frac{-\alpha_{ij} N_j^*}{1 + \sum_l \alpha_{il} N_l^*} \end{cases}$$

Let's define $f_A(i) = \sum_l \alpha_{ij} N_l^*$.

$$b_{ij}(1 + f_A(i)) = -\alpha_{ij} N_j^*$$

We then sum on columns (on j).

$$\sum_j [b_{ij}(1 + f_A(i))] = -f_A(i)$$

$$\Leftrightarrow -f_A(i)(1 + \sum_j b_{ij}) = \sum_j b_{ij}$$

$$\Leftrightarrow f_A(i) = -\frac{\sum_j b_{ij}}{(1 + \sum_j b_{ij})}$$

$$\Leftrightarrow \alpha_{ij} = -\frac{1}{N_j^*} b_{ij}(1 - \frac{\sum_j b_{ij}}{1 + \sum_j b_{ij}})$$

$$\Leftrightarrow \alpha_{ij} = -\frac{1}{N_j^*} \frac{b_{ij}}{1 + \sum_j b_{ij}}$$

This gives an exact correspondance between α_{ij} and b_{ij}.

Quadratic programming

The quadratic programming algorithm aims at finding $\mathbf{x}$ that minimizes $||\mathbf{Cx} - \mathbf{d}||^2$ under the constraints $\mathbf{Ex} = \mathbf{f}$ and $\mathbf{Gx} >= \mathbf{h}$.

Here, $\mathbf{C} = \mathbf{I}$, $\mathbf{d} = [\text{vec}(\mathbf{A}^T)\frown\mathbf{r}']$ where $\mathbf{A}$ is the interaction matrix, $\mathbf{r}' = -(e^{\mathbf{r}} - \mathbf{1})$ is the vector of growth rates, $\mathbf{E}$ is built so that we verify the equality $\mathbf{AN}^* + \mathbf{r}' = 0$ where $\mathbf{N}^*$ is the vector of abundance at equilibrium (more precisely, here, average abundance values over the whole time series), and $\mathbf{G}, \mathbf{h}$ so that $\mathbf{r} > 0$ (genera have a positive growth rate when taken in isolation) and $\forall i, a_{ii} > 0$ (negative density-dependence, individuals from the same genus compete with each other).

NOTE: This may not be useful as only the mean growth rate can be used to adjust the model (due to its dependence on the temperature), and the calibration of the interaction matrix tends to lead to a stable community, that is not able to represent the yearly cycles due to seasonality.

Mortality in the sediment

McQuoid *et al.* (2002) present maximum and mean depth at which germination of diatoms and dinoflagellates occurred in sediments. They also present sediment datation according to depth. Depth can therefore be related to maximum and mean age of phytoplankton before death.

Assuming m is the probability of mortality, m follows a geometric law, i.e., m is the probability distribution of the number of days needed for a phytoplankon cyst to die. The expectancy for the life duration (the number of days without dying) is $\frac{1}{m} \Leftrightarrow m = \frac{1}{L_{mean}}$ where L_{mean} is the average life duration.

Another way to look at the process is that life expectancy L follows the distribution $p(L > l) = e^{-ml}$. With maximum values, we can arbitrarily choose that for these values $p(L > l_{max}) = 0.05$. In this, $m = -\frac{ln(p(L > l_{max}))}{l_{max}}$.

In both cases, $m \propto 10^{-4}\text{d}^{-1}$.

References

Agrawal, S.C. (2009). Factors affecting spore germination in algae - review. *Folia Microbiologica*, 54, 273–302.

Ascione Kenov, I., Muttin, F., Campbell, R., Fernandes, R., Campuzano, F., Machado, F., Franz, G. & Neves, R. (2015). Water fluxes and renewal rates at Pertuis d'Antioche/Marennes-Oléron Bay, France. *Estuarine, Coastal and Shelf Science*, 167, 32–44.

Balzano, S., Sarno, D. & Kooistra, W.H.C.F. (2011). Effects of salinity on the growth rate and morphology of ten Skeletonema strains. *Journal of Plankton Research*, 33, 937–945.

Bazaraa, M.S., Sherali, H.D. & Shetty, C.M. (2013). *Nonlinear programming: theory and algorithms*. John Wiley & Sons.

Bissinger, J., Montagnes, D., Harples, J. & Atkinson, D. (2008). Predicting marine phytoplankton maximum growth rates from temperature: Improving on the Eppley curve using quantile regression. *Limnology and Oceanography*, 53, 487–493.

Cáceres, C.E. (1997). Temporal variation, dormancy, and coexistence: A field test of the storage effect. *Proceedings of the National Academy of Sciences*, 94, 9171–9175.

Certain, G., Barraquand, F. & Gåardmark, A. (2018). How do MAR(1) models cope with hidden nonlinearities in ecological dynamics? *Methods in Ecology and Evolution*, 9, 1975–1995.

Chesson, P. (1986). Environmental variation and the coexistence of species. In: *Community ecology* (eds. Diamond, J. & Case, T.). Harper & Row, New-York, chap. 14, pp. 240–256.

Comita, L., Queenborough, S., Murphy, S., Eck, J., Xu, K., Krishnadas, M., Beckman, N. & Zhu, Y. (2014). Testing predictions of the Janzen-Connell hypothesis: a meta-analysis of experimental evidence for distance- and density-dependent seed and seedling survival. *Journal of Ecology*, 102, 845–856.

Edwards, K., Thomas, M., Klausmeier, C. & Litchman, E. (2015). Light and growth in marine phytoplankton: allometric, taxonomic, and environmental variation. *Limnology and Oceanography*, 60, 540–552.

Edwards, K., Thomas, M., Klausmeier, C. & Litchman, E. (2016). Phytoplankton growth and the interaction of light and temperature: A synthesis at the species and community level. *Limnology and Oceanography*, 61, 1232–1244.

Eilertsen, H., Sandberg, S. & Tøllefsen, H. (1995). Photoperiodic control of diatom spore growth; a theory to explain the onset of phytoplankton blooms. *Marine Ecology Progress Series*, 116, 303–307.

Ellegaard, M. & Ribeiro, S. (2018). The long-term persistence of phytoplankton resting stages in aquatic `seed banks'. *Biological Reviews*, 93, 166–183.

Ellner, S., Snyder, R. & Adler, P. (2016). How to quantify the temporal storage effect using simulations instead of math. *Ecology Letters*, 19, 1333–1342.

Eppley, R. (1972). Temperature and phytoplankton growth in the sea. *Fishery Bulletin*, 70, 1063–1085.

Fransz, H. & Verhagen, J. (1985). Modelling research on the production cycle of phytoplankton in the Southern Bight of the North Sea in relation to riverborne nutrient loads. *Netherlands Journal of Sea Research*, 19, 241–250.

Hinners, J., Hense, I. & Kremp, A. (2019). Modelling phytoplankton adaptation to global warming based on resurrection experiments. *Ecological Modelling*, 400, 27–33.

Kowe, R., Skidmore, R., Whitton, B. & Pinder, A. (1998). Modelling phytoplankton dynamics in the River Swale, an upland river in NE England. *Science of The Total Environment*, 210, 535–546.

Le Pape, O., Jean, F. & Ménesguen, A. (1999). Pelagic and benthic trophic chain coupling in a semi-enclosed coastal system, the Bay of Brest (France): a modelling approach. *Marine Ecology Progress Series*, 189, 135–147.

Marcus, N. & Boero, F. (1998). Minireview: The importance of benthic-pelagic coupling and the forgotten role of life cycles in coastal aquatic systems. *Limnology and Oceanography*, 43, 763–768.

Maynard, D.S., Wootton, J.T., Serván, C.A. & Allesina, S. (2019). Reconciling empirical interactions and species coexistence. *Ecology Letters*, 22, 1028–1037.

McQuoid, M.R., Godhe, A. & Nordberg, K. (2002). Viability of phytoplankton resting stages in the sediments of a coastal Swedish fjord. *European Journal Phycology*, 37, 191–201.

Nguyen, V., Buckley, Y.M., Salguero-Gómez, R. & Wardle, G.M. (2019). Consequences of neglecting cryptic life stages from demographic models. *Ecological Modelling*, 408, 108723.

Passow, U. (1991). Species-specific sedimentation and sinking velocities of diatoms. *Marine Biology*, 108, 449–455.

Patrick, R. (1948). Factors effecting the distribution of diatoms. *Botanical Review*, 14, 473–524.

Picoche, C. & Barraquand, F. (2019). How self-regulation, the storage effect, and their interaction contribute to coexistence in stochastic and seasonal environments. *Theoretical Ecology*.

Picoche, C. & Barraquand, F. (2020). Strong self-regulation and widespread facilitative interactions between genera of phytoplankton. preprint, bioRxiv.

Reynolds, C.S. (2006). *The ecology of phytoplankton*. Cambridge University Press.

Sanyal, A., Larsson, J., van Wirdum, F., Andrén, T., Moros, M., Lönn, M. & Andrén, E. (2018). Not dead yet: Diatom resting spores can survive in naturefor several millennia. preprint, bioRxiv.

Scranton, K. & Vasseur, D.A. (2016). Coexistence and emergent neutrality generate synchrony among competitors in fluctuating environments. *Theoretical Ecology*, 9, 353–363.

Shoemaker, L.G. & Melbourne, B.A. (2016). Linking metacommunity paradigms to spatial coexistence mechanisms. *Ecology*, 97, 2436–2446.

Smayda, T.J. (2002). Turbulence, watermass stratification and harmful algal blooms: an alternative view and frontal zones as "pelagic seed banks". *Harmful Algae*, 1, 95–112.

Wiedmann, I., Reigstad, M., Marquardt, M., Vader, A. & Gabrielsen, T. (2016). Seasonality of vertical flux and sinking particle characteristics in an ice-free high arctic fjord-Different from subarctic fjords? *Journal of Marine Systems*, 154, 192–205.

Wisnoski, N.I., Leibold, M.A. & Lennon, J.T. (2019). Dormancy in metacommunities. *The American Naturalist*, 194, 135–151.